Joint Design of Fronthaul and Access Links in Massive MIMO Multi-UAV-enabled CRANs

Yingjia Huang and Aissa Ikhlef, *Senior Member, IEEE*

***Abstract*—This paper proposes a novel architecture of multi-unmanned aerial vehicle (UAV)-enabled cloud radio access network (CRAN). In particular, we propose to deploy the UAVs as flying remote radio heads (RRHs) to serve ground user equipments (UEs). The baseband unit (BBU) is equipped with a large-scale antenna array to serve the flying RRHs and affords all the baseband signal processing. To optimize the proposed architecture, we consider the maximization of the minimum rate of UEs by jointly optimizing UAVs placement, quantization noise variance, and power control. The corresponding optimization problem is not convex and to solve it we devise an efficient iterative algorithm combining the block coordinate descent and successive convex optimization methods. Numerical results demonstrate the superior performance of the proposed algorithm compared to two benchmark schemes.**

***Index Terms*—CRAN, UAV-enabled communication, massive MIMO, power control, UAV placement.**

I. Introduction

Unmanned aerial vehicles (UAVs) are regarded as a good candidate for temporary network deployment and coverage extension due to their low cost, fast deployment, dynamic adjustment, and adaptability in severe environment and difficult-to-reach areas [1]–[3]. Particularly, UAV-aided communications are indispensable in some situations where conventional terrestrial communication systems are overloaded or even nonexistent, for instance, temporary network coverage of major sports events or emergency network coverage in disaster scenarios [4]. Compared with terrestrial communications, there is a higher possibility for air-to-ground channels that are mainly dominated by line-of-sight (LoS) components [5]. This is beneficial to UAV-enabled communication to achieve a stable connection and quality-of-service requirements.

However, the constrained flying time is a critical shortcoming due to the UAVs' limited battery capacity. The cloud radio access network (CRAN) framework is a promising solution to this challenge. Inspired by the centralized signal processing technology, the CRAN architecture moves most of the processing and computation from the traditional base stations (BSs) to the baseband unit (BBU) resulting in improved spectral and energy efficiencies [6]. In CRAN, the BSs are called remote radio heads (RRHs) and operate as distributed radio frequency (RF) transceivers. The BBU communicates with the RRHs through the fronthaul links while the RRHs communicate with the user equipments (UEs) via the access links.

Yingjia Huang and Aissa Ikhlef are with the Department of Engineering, Durham University, Durham, DH1 3LE, United Kingdom (email: {yingjia.huang, aissa.ikhlef}@durham.ac.uk.)

This work was supported by the UK Engineering and Physical Sciences Research Council under Grant EP/R044090/1.

Motivated by the benefits of CRAN, we propose a new architecture by deploying UAVs as flying RRHs and using a large-scale antenna array at the BBU[1]. Thanks to the centralized processing, the use of massive MIMO at the BBU, and the inherent LoS fronthaul links, this architecture will allow the energy-limited UAVs to have lower signal processing complexity, lower cost, lower power consumption and thus longer service and flying times. The proposed system is very promising in some practical scenarios such as disaster management (e.g., when terrestrial networks are non-existent, overloaded, or damaged), temporary events coverage (e.g., major sporting and other public events), and coverage extension (e.g., range extension of cellular networks and coverage of non-reachable areas by terrestrial communication systems). In particular, it can realize temporary and cost-effective communication requirement with fast deployment, dynamic adjustment, and wide-range coverage under these scenarios.

The use of multi-UAV-enabled wireless communication systems with centralized signal processing was considered in [7]–[10]. [7] studied coordinated multipoint (CoMP) in CRAN by using UAVs as RRHs and dynamically optimized the UAV placement for max-min rate fairness. [8] considered multi-UAV trajectory control to maximize the minimum rate. In both [7] and [8] the fronthaul links were assumed to have unlimited/very high capacity. [9] maximized the sum-rate in the uplink of CRAN with LoS fronthaul and access links by optimizing the UE association, UAV placement, and UEs' and UAVs' transmit powers. However, both the fronthaul and access links were assumed to be interference-free by using orthogonal frequency bands for different users. The authors in [10] maximized the sum-rate, where UAVs are deployed as relays assuming that the direct links between the single-antenna BS and UEs are blocked. In our work, unlike the existing works, we adopt a more realistic system model with a massive MIMO BBU and a decompress-and-forward (DCF) relaying protocol at the flying RRHs and jointly optimize both the fronthaul and access links including the placements of the UAVs. To the best of the authors' knowledge, this work is the first to use massive MIMO and compression at the BBU and DCF at the flying RRHs to improve the capacity of the wireless fronthaul links in multi-UAV-enabled CRANs, where usually the fronthaul link is the bottleneck.

The remainder of this paper is organized as follows. In Section II, we introduce the system model. The max-min fairness optimization problem and its solution are presented in Section III. Section IV provides numerical results to verify the

[1]As a result, the proposed architecture will inherit all the benefits of the conventional CRAN architecture.

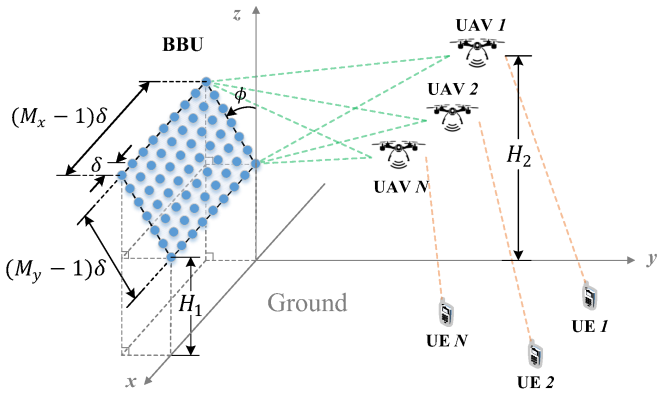

Fig. 1. System model of the proposed UAV-enabled CRAN.

effectiveness of the proposed system. Finally, the conclusion is drawn in Section V.

II. System Model

We consider the downlink transmission in a UAV-enabled CRAN system consisting of $N > 1$ single-antenna UE and single-antenna UAV pairs[2]. We assume that the BBU is equipped with a large-scale uniform planar array (UPA) of $M \gg N$ antennas. We adopt the time division duplex (TDD) transmission mode to coordinate the transmissions among the fronthaul and access links[3]. We assume that direct links between the BBU and the UEs do not exist or are too weak, and hence are not exploited for simplicity of implementation. Fig. 1 shows the geometric model of the system. We establish a 3D coordinate system (x, y, z) where the ground is set as the x-y plane. One corner antenna of UPA is located at $(0, 0, H_B)$, where H_B is the BBU height. We assume that the UPA is equipped with M_y rows of antennas where all the rows are parallel with the x-axis. Each row has M_x antennas with an antenna spacing $\delta = \lambda/2$, where λ is the wavelength. Hence, the total number of antennas at the BBU is $M = M_x M_y$. For notational convenience, we define the antenna element in the ith column, $i \in \{1, \ldots, M_x\}$, and the jth row, $j \in \{1, \ldots, M_y\}$ as the mth antenna where $m = i + (j-1)M_x$. Also, we define $\mathcal{K}_{\mathrm{R}} = \{1, \ldots, N\}$, $\mathcal{K}_{\mathrm{U}} = \{1, \ldots, N\}$ and $\mathcal{K}_{\mathrm{B}} = \{1, \ldots, M\}$ as the sets of UAVs, UEs, and the antennas at the BBU, respectively. Based on this coordinate system, the location of the mth antenna is defined as $\mathbf{v}_{\mathrm{B},m} = ((i-1)\delta, -(j-1)\delta \sin\phi, (j-1)\delta\cos\phi + H_B)$, where ϕ is the inclined angle between the array and the x-z plane as shown in Fig. 1. We assume that the UAVs fly at a constant altitude H_R. We define the locations of the ith UAV and the jth UE as $\boldsymbol{q}_i = (x_i, y_i, H_R), i \in \mathcal{K}_{\mathrm{R}}$ and $\mathbf{v}_{\mathrm{U},j} = (x_{\mathrm{U},j}, y_{\mathrm{U},j}, 0), j \in \mathcal{K}_{\mathrm{U}}$, respectively. We assume that the locations of UEs are constant and perfectly known. Hence, the distance d_{ij} between UAV i and UE j is $d_{ij} = ||\boldsymbol{q}_i - \mathbf{v}_{\mathrm{U},j}|| = \sqrt{(x_i - x_{\mathrm{U},j})^2 + (y_i - y_{\mathrm{U},j})^2 + H_R^2}$, and distance l_{mi} between the mth BBU antenna element and the ith UAV is $l_{mi} = \|\boldsymbol{q}_i - \mathbf{v}_{\mathrm{B},m}\|$.

Let $\boldsymbol{g}_i \triangleq [g_{1i}, \ldots, g_{Mi}]^T$ and $\boldsymbol{h}_j \triangleq [h_{1j}, \ldots, h_{Nj}]^T$ denote the downlink channel coefficients from all antennas at the BBU to the ith UAV and from all UAVs to the jth UE, respectively. $(\cdot)^T$ denotes the transpose operation. Since the ground-to-air and air-to-ground channels are generally dominated by the LoS link in practice, for simplicity, we assume that both the fronthaul and access links are modeled as LoS channels [7], [11]. As a result, the channels between the mth BBU antenna and the ith UAV and between the ith UAV and the jth UE are defined as $g_{mi} = \sqrt{\frac{\xi}{l_{mi}^2}}\bar{g}_{mi}$ and $h_{ij} = \sqrt{\frac{\xi}{d_{ij}^2}}\bar{h}_{ij}$, respectively. $\bar{g}_{mi} = e^{-\mathrm{i}\frac{2\pi}{\lambda}l_{mi}}$, $\bar{h}_{ij} = e^{-\mathrm{i}\frac{2\pi}{\lambda}d_{ij}}$, and ξ represents the path loss at the reference distance $d_0 = 1$m in both links. For future use, we define $\bar{\boldsymbol{g}}_i \triangleq [\bar{g}_{1i}, \ldots, \bar{g}_{Mi}]^T$.

Let $\tilde{u}_{\mathrm{R},i} = \sqrt{p_i}s_{\mathrm{U},i}$ denote the signal that the BBU intends to transmit to the ith UE where $s_{\mathrm{U},i} \sim \mathcal{CN}(0,1)$ and p_i is the power of $\tilde{u}_{R,i}$. The BBU first quantizes and compresses $\tilde{u}_{\mathrm{R},i}$. We adopt the decompress-and-forward relaying strategy and use the Gaussian quantization test channel to model the quantization process [12]. Hence, the resulting quantized signal, $u_{\mathrm{R},i}$, can be expressed as

$$u_{\mathrm{R},i} = \tilde{u}_{\mathrm{R},i} + t_i, \tag{1}$$

where $t_i \sim \mathcal{CN}(0, \Omega_i)$ is the compression noise. By assuming that the signals $\tilde{u}_{\mathrm{R},i}$, $i \in \mathcal{K}_{\mathrm{U}}$, are compressed independently, their corresponding quantization noises are hence uncorrelated, i.e., $\mathbb{E}[t_i t_j^*] = 0$ for $i \neq j$ [12]. Let $\boldsymbol{\Omega} = [\Omega_1, \ldots, \Omega_N]^T$. The BBU then compresses the quantized signal $u_{\mathrm{R},i}$ to generate the compression index $U_i \in \left\{1, \ldots, 2^{nC_i}\right\}$, where n denotes the coding block length and C_i denotes the rate of message U_i. Subsequently, the BBU encodes each message U_i to obtain the encoded baseband signal $s_{\mathrm{R},i} \sim \mathcal{CN}(0,1)$ and generates the precoding vector $\mathbf{v}_i = \sqrt{\eta_i}\mathbf{w}_i \in \mathbb{C}^{M\times 1}$, where η_i is a real-valued coefficient and $\mathbf{w}_i$ is the ith column of the precoding matrix $\mathbf{W} \in \mathbb{C}^{M\times N}$. We consider the zero-forcing (ZF) precoding method where $\mathbf{W}$ is defined as

$$\mathbf{W} = \bar{\mathbf{G}}^* \left(\bar{\mathbf{G}}^T \bar{\mathbf{G}}^*\right)^{-1} \tag{2}$$

where $\bar{\mathbf{G}} \triangleq [\bar{\boldsymbol{g}}_1, \ldots, \bar{\boldsymbol{g}}_N]$ and $(\cdot)^*$ is the complex conjugate. Next, the BBU sends the precoded signal $\sum_{i\in\mathcal{K}_{\mathrm{R}}} \mathbf{w}_i\sqrt{\eta_i}s_{\mathrm{R},i}$ to the UAVs. The signal received by the ith UAV is given by

$$y_{\mathrm{R},i} = \boldsymbol{g}_i^T\mathbf{w}_i\sqrt{\eta_i}s_{\mathrm{R},i} + \boldsymbol{g}_i^T \sum_{k\in\mathcal{K}_{\mathrm{R}}\setminus\{i\}} \mathbf{w}_k\sqrt{\eta_k}s_{\mathrm{R},k} + z_i, \tag{3}$$

where $z_i \sim \mathcal{CN}(0, \sigma_R^2)$ denotes the noise at the ith UAV, $i \in \mathcal{K}_{\mathrm{R}}$. Therefore, the rate C_i through the fronthaul link should be constrained as

$$C_i \leq f_{\mathrm{front},i}(\mathbf{Q}, \boldsymbol{\eta}) \triangleq \log_2\left(1 + \frac{\eta_i \left|\boldsymbol{g}_i^T\mathbf{w}_i\right|^2}{\sum\limits_{k\in\mathcal{K}_{\mathrm{R}}\setminus\{i\}} \eta_k \left|\boldsymbol{g}_i^T\mathbf{w}_k\right|^2 + \sigma_R^2}\right), \tag{4}$$

where $\mathbf{Q} = \left[\boldsymbol{q}_1^T, \ldots, \boldsymbol{q}_N^T\right]^T$ and $\boldsymbol{\eta} = [\eta_1, \ldots, \eta_N]^T$. Then, each UAV i decompresses the signal received from the BBU to recover the message $u_{\mathrm{R},i}$. In order to decompress the signals successfully at the UAVs, the message rate C_i should be bounded as [13]

$$C_i \geq f_{\mathrm{compress},i}(p_i, \Omega_i) \triangleq \log_2\left(1 + \frac{p_i}{\Omega_i}\right), \; i \in \mathcal{K}_{\mathrm{R}}. \tag{5}$$

[2]We note that a UAV can serve multiple UEs via using multiple access techniques such as frequency division multiple access (FDMA), time division multiple access (TDMA), code division multiple access (CDMA), orthogonal frequency division multiple access (OFDMA), etc.

[3]Note that the investigation of the signalling overheads among the BBU, UAVs, and UEs as well as their costs and timeliness is beyond the scope of this letter.

The message recovered by UAV i, $u_{\mathrm{R},i}$, is then forwarded to its paired UE i. The signal received by the ith UE is given by

$$y_{\mathrm{U},i} = h_{ii}\sqrt{p_i}s_{\mathrm{U},i} + \sum_{j\in\mathcal{K}_\mathrm{R}\setminus\{i\}} h_{ji}\sqrt{p_j}s_{\mathrm{U},j} + \sum_{j\in\mathcal{K}_\mathrm{R}} h_{ji}t_j + n_i, \quad (6)$$

where $n_i \sim \mathcal{CN}(0,\sigma_U^2)$ denotes the noise at UE i. Hence, the achievable rate for UE i can be obtained as

$$\mathcal{R}_j\left(\mathbf{Q},\boldsymbol{p},\boldsymbol{\Omega}\right) \triangleq \mathcal{R}_{j,1} - \mathcal{R}_{j,2}, \quad (7)$$

where

$$\mathcal{R}_{j,1} = \log_2\Big(\sum_{i\in\mathcal{K}_\mathrm{R}} \left(p_i+\Omega_i\right)\left|h_{ij}\right|^2 + \sigma_U^2\Big), \quad (8)$$

$$\mathcal{R}_{j,2} = \log_2\Big(\sum_{i\in\mathcal{K}_\mathrm{R}\setminus\{j\}} p_i\left|h_{ij}\right|^2 + \sum_{i\in\mathcal{K}_\mathrm{R}} \Omega_i\left|h_{ij}\right|^2 + \sigma_U^2\Big). \quad (9)$$

In the next section, we jointly optimize the power control coefficients, the quantization noise variance, and the UAV placement according to the max-min fairness criterion[4].

III. Max-min fairness

In this section, our goal is to maximize the minimum rate among all UEs via the optimization of UAVs placement $\mathbf{Q}$, power control $\boldsymbol{\eta},\boldsymbol{p}$, and quantization noise variance $\boldsymbol{\Omega}$. According to (4), (5), and (7), the corresponding optimization problem can be formulated as

$$\max_{\mathbf{Q},\boldsymbol{\eta},\boldsymbol{p},\boldsymbol{\Omega},\boldsymbol{C}} \ \min_j \ \mathcal{R}_j\left(\mathbf{Q},\boldsymbol{p},\boldsymbol{\Omega}\right), \ \forall j\in\mathcal{K}_\mathrm{U}, \quad (10a)$$

$$\text{s.t.} \quad C_i \le f_{\text{front},i}(\mathbf{Q},\boldsymbol{\eta}), \ \forall i\in\mathcal{K}_\mathrm{R}, \quad (10b)$$

$$C_i \ge f_{\text{compress},i}(p_i,\Omega_i), \ \forall i\in\mathcal{K}_\mathrm{R}, \quad (10c)$$

$$p_i+\Omega_i \le P_{R,i}, \ \forall i\in\mathcal{K}_\mathrm{R}, \quad (10d)$$

$$\mathrm{tr}\left\{\mathrm{diag}\left(\eta_1,\ldots,\eta_K\right)\mathbf{W}^H\mathbf{W}\right\} \le P_B, \quad (10e)$$

$$\left\|\boldsymbol{q}_i-\boldsymbol{q}_k\right\|^2 \ge d_{\min}^2, \ \forall i,k\in\mathcal{K}_\mathrm{R}, \ i\ne k, \quad (10f)$$

$$\eta_i\ge 0, \ p_i\ge 0, \ \Omega_i\ge 0, \ \forall i\in\mathcal{K}_\mathrm{R}, \quad (10g)$$

where $\boldsymbol{C} \triangleq [C_1,\ldots,C_N]^T$ and $d_{\min}$ is the minimum safety distance between any two UAVs to avoid collisions. (10d) and (10e) refer to the power constraints at each UAV and the BBU, respectively. $P_{R,i}$ and P_B denote the maximum transmit powers at RRH i and BBU, respectively. $(\cdot)^H$ denote the conjugate transpose.

It is clear that problem (10) is very hard to solve because it is nonconvex. To solve it, we propose to decompose it into two convex sub-problems and solve them iteratively by applying the block coordinate descent and successive convex optimization method [11].

A. Sub-Problem 1: UAV placement optimization

Firstly, for any given $\boldsymbol{\eta},\boldsymbol{p},\boldsymbol{\Omega}$, we aim to optimize the UAV placement $\mathbf{Q}$. Therefore, sub-problem 1 is derived from problem (10) as

$$\max_{\mathbf{Q},\boldsymbol{C}} \ \min_j \ \mathcal{R}_{j,1}\left(\mathbf{Q}\right) - \mathcal{R}_{j,2}\left(\mathbf{Q}\right) \quad (11a)$$

$$\text{s.t.} \quad C_i \le f_{\text{front},i}(\mathbf{Q}), \ \forall i\in\mathcal{K}_\mathrm{R}, \quad (11b)$$

$$C_i \ge f_{\text{compress},i}, \ \forall i\in\mathcal{K}_\mathrm{R}, \quad (11c)$$

$$\left\|\boldsymbol{q}_i-\boldsymbol{q}_k\right\|^2 \ge d_{\min}^2, \ \forall i,k\in\mathcal{K}_\mathrm{R}, \ i\ne k. \quad (11d)$$

[4]Note that it is straightforward to extend this work to other criteria such as the sum-rate criterion.

It is observed that the objective function (11a) and constraints (11b) and (11c) are all non-convex. Define slack variables $\mathbf{S} \triangleq \{S_{ij}, \ \forall i\in\mathcal{K}_\mathrm{R}, j\in\mathcal{K}_\mathrm{U}\}$. Then, $\mathcal{R}_{j,2}$ in (9) can equivalently be rewritten as

$$\mathcal{R}_{j,2}(\mathbf{S}) = \log_2\left(\xi\sum_{i\in\mathcal{K}_\mathrm{R}\setminus\{j\}}\frac{p_i+\Omega_i}{S_{ij}} + \xi\frac{\Omega_j}{S_{jj}} + \sigma_R^2\right). \quad (12)$$

Thus, problem (11) can be recast as

$$\max_{\mathbf{Q},\mathbf{S},\boldsymbol{C}} \ \min_j \ \mathcal{R}_{j,1}\left(\mathbf{Q}\right) - \mathcal{R}_{j,2}\left(\mathbf{S}\right) \quad (13a)$$

$$\text{s.t.} \quad S_{ij} \le \left\|\boldsymbol{q}_i-\mathbf{v}_{\mathrm{U},j}\right\|^2, \ \forall i\in\mathcal{K}_\mathrm{R}, j\in\mathcal{K}_\mathrm{U}, \quad (13b)$$

$$(11\text{b}), \ (11\text{c}), \ (11\text{d}).$$

Note that $\mathcal{R}_{j,1}\left(\mathbf{Q}\right)$ is neither convex nor concave with respect to $\boldsymbol{q}_i$, but it is convex with respect to $\left\|\boldsymbol{q}_i-\mathbf{v}_{\mathrm{U},j}\right\|^2$. Define $\boldsymbol{q}_i^{(r)} = \left\{\boldsymbol{q}_i^{(r)}, \forall i\in\mathcal{K}_\mathrm{R}\right\}$ as the placement solution from the $(r-1)$th iteration. By taking the first-order Taylor expansion at the point $\left\|\boldsymbol{q}_i^{(r)}-\mathbf{v}_{\mathrm{U},j}\right\|^2$, we can get the lower bound for $\mathcal{R}_{j,1}$ with respect to $\left\|\boldsymbol{q}_i-\mathbf{v}_{\mathrm{U},j}\right\|^2$ as

$$\begin{aligned}\mathcal{R}_{j,1} &= \log_2\Big(\xi\sum_{i\in\mathcal{K}_\mathrm{R}}\frac{p_i+\Omega_i}{\left\|\boldsymbol{q}_i-\mathbf{v}_{\mathrm{B},j}\right\|^2}+\sigma_U^2\Big)\\ &\ge \sum_{i\in\mathcal{K}_\mathrm{R}} -A_{j,i}^{(r)}\left(\left\|\boldsymbol{q}_i-\mathbf{v}_{\mathrm{B},j}\right\|^2-\left\|\boldsymbol{q}_i^{(r)}-\mathbf{v}_{\mathrm{B},j}\right\|^2\right)+B_j^{(r)}\\ &\triangleq \mathcal{R}_{j,1}^{\text{lb}}, \ \forall j\in\mathcal{K}_\mathrm{U}, \end{aligned} \quad (14)$$

where $A_{j,i}^{(r)} = \frac{\xi(p_i+\Omega_i)\log_2 e}{\left\|\boldsymbol{q}_i^{(r)}-\mathbf{v}_{\mathrm{B},j}\right\|^4\left(\sum\limits_{k\in\mathcal{K}_\mathrm{R}}\frac{\xi(p_k+\Omega_k)}{\left\|\boldsymbol{q}_k^{(r)}-\mathbf{v}_{\mathrm{B},j}\right\|^2}+\sigma_U^2\right)}$, and $B_j^{(r)} = \log_2\left(\sum\limits_{k\in\mathcal{K}_\mathrm{R}}\frac{\xi(p_k+\Omega_k)}{\left\|\boldsymbol{q}_k^{(r)}-\mathbf{v}_{\mathrm{B},j}\right\|^2}+\sigma_U^2\right)$ are constants.

Since the antenna spacing at the BBU is negligible compared with the distance between the BBU and UAVs, it is reasonable to assume that all the links to the same UAV are identical and hence $l_{mi}\approx l_i$, $\forall m\in\mathcal{K}_\mathrm{B}$. Given the ZF precoder in (2), this results in $\sum\limits_{k\in\mathcal{K}_\mathrm{R}\setminus\{i\}}\eta_k\left|\boldsymbol{g}_i^T\mathbf{w}_k\right|^2 = 0$ in (4. Thus, the fronthaul achievable rate $f_{\text{front},i}(\mathbf{Q})$ in (4) can be reexpressed as

$$f_{\text{front},i}(\boldsymbol{q}_i) = \log_2\left(1+\frac{\xi\eta_i}{\sigma_R^2\left\|\boldsymbol{q}_i-\mathbf{v}_{\mathrm{U},1}\right\|^2}\right), \quad (15)$$

which is convex with respect to $\left\|\boldsymbol{q}_i-\mathbf{v}_{\mathrm{U},1}\right\|^2$ but constraint (11b) is still non-convex. Therefore, we derive the lower bound at the point $\left\|\boldsymbol{q}_i^{(r)}-\mathbf{v}_{\mathrm{U},1}\right\|^2$, $\forall i\in\mathcal{K}_\mathrm{R}$, which is given by

$$\begin{aligned}f_{\text{front},i}(\boldsymbol{q}_i) &\ge -C_i^{(r)}\left(\left\|\boldsymbol{q}_i-\mathbf{v}_{\mathrm{U},1}\right\|^2-\left\|\boldsymbol{q}_i^{(r)}-\mathbf{v}_{\mathrm{U},1}\right\|^2\right)+D_i^{(r)}\\ &\triangleq f_{\text{front},i}^{\text{lb},1}(\boldsymbol{q}_i),\end{aligned} \quad (16)$$

where $C_i^{(r)} = \frac{\eta_i\log_2 e}{\frac{\sigma_R^2}{\xi}\left\|\boldsymbol{q}_i^{(r)}-\mathbf{v}_{\mathrm{U},1}\right\|^4+\eta_i\left\|\boldsymbol{q}_i^{(r)}-\mathbf{v}_{\mathrm{U},1}\right\|^2}$ and $D_i^{(r)} = \log_2\left(1+\frac{\xi\eta_i}{\sigma_R^2\left\|\boldsymbol{q}_i^{(r)}-\mathbf{v}_{\mathrm{U},1}\right\|^2}\right)$ are constants. Similarly, $\left\|\boldsymbol{q}_i-\mathbf{v}_{\mathrm{U},j}\right\|^2$ is convex with respect to $\boldsymbol{q}_i$, hence constraint (13b) is non-convex. By applying the first-order Taylor expansion, the lower bound of $\left\|\boldsymbol{q}_i-\mathbf{v}_{\mathrm{U},j}\right\|^2$ at $\boldsymbol{q}_i^{(r)}$ is given by

$$\left\|\boldsymbol{q}_i-\mathbf{v}_{\mathrm{U},j}\right\|^2 \ge \left\|\boldsymbol{q}_i^{(r)}-\mathbf{v}_{\mathrm{U},j}\right\|^2+2(\boldsymbol{q}_i^{(r)}-\mathbf{v}_{\mathrm{U},j})^T(\boldsymbol{q}_i-\boldsymbol{q}_i^{(r)}). \quad (17)$$

Also, we can get the lower bound for the $\left\|\boldsymbol{q}_i-\boldsymbol{q}_j\right\|^2$ in constraint (11d) as

$$\left\|\boldsymbol{q}_i-\boldsymbol{q}_k\right\|^2 \ge -\left\|\boldsymbol{q}_i^{(r)}-\boldsymbol{q}_k^{(r)}\right\|^2+2(\boldsymbol{q}_i^{(r)}-\boldsymbol{q}_k^{(r)})^T(\boldsymbol{q}_i-\boldsymbol{q}_k). \quad (18)$$

Now, using (14)-(18), problem (11) can be reformulated as

$$\max_{\mathbf{Q},\mathbf{S},\boldsymbol{C}} \quad \min_{j} \ \mathcal{R}^{\text{lb}}_{j,1}(\mathbf{Q}) - \mathcal{R}_{j,2}(\mathbf{S}) \tag{19a}$$

$$\text{s.t.} \quad S_{ij} \le \|\boldsymbol{q}_i^{(r)} - \mathbf{v}_{\text{U},j}\|^2 + 2\big(\boldsymbol{q}_i^{(r)} - \mathbf{v}_{\text{U},j}\big)^T \times \big(\boldsymbol{q}_i - \boldsymbol{q}_i^{(r)}\big),\ \forall i \in \mathcal{K}_{\text{R}}, j \in \mathcal{K}_{\text{U}}, \tag{19b}$$

$$C_i \le f^{\text{lb},1}_{\text{front},i}(\boldsymbol{q}_i),\ \forall i \in \mathcal{K}_{\text{R}}, \tag{19c}$$

$$d^2_{\min} \le -\|\boldsymbol{q}_i^{(r)} - \boldsymbol{q}_k^{(r)}\|^2 + 2\big(\boldsymbol{q}_i^{(r)} - \boldsymbol{q}_k^{(r)}\big)^T \times \big(\boldsymbol{q}_i - \boldsymbol{q}_k\big),\ \forall i,k \in \mathcal{K}_{\text{R}},\ i \ne k, \tag{19d}$$

(11c),

which is a convex problem and can thus be solved iteratively using a standard convex optimization toolbox such as CVX [14].

B. Sub-Problem 2: Power control and quantization noise variance optimization

Now, for any given UAV placement $\mathbf{Q}$, we aim to optimize the power coefficients $\boldsymbol{\eta}, \boldsymbol{p}$ and quantization noise $\boldsymbol{\Omega}$. From problem (10), we can obtain sub-problem 2 as follows

$$\max_{\boldsymbol{\eta},\boldsymbol{p},\boldsymbol{\Omega},\boldsymbol{C}} \quad \min_{j} \ \mathcal{R}_{j,1}(\boldsymbol{p},\boldsymbol{\Omega}) - \mathcal{R}_{j,2}(\boldsymbol{p},\boldsymbol{\Omega}) \tag{20a}$$

$$\text{s.t.} \quad C_i \le f_{\text{front},i}(\boldsymbol{\eta}),\ \forall i \in \mathcal{K}_{\text{R}}, \tag{20b}$$

$$C_i \ge f_{\text{compress},i}(p_i, \Omega_i),\ \forall i \in \mathcal{K}_{\text{R}}, \tag{20c}$$

$$p_i + \Omega_i \le P_{R,i},\ \forall i \in \mathcal{K}_{\text{R}}, \tag{20d}$$

$$\text{tr}\left\{\text{diag}\left(\eta_1, \ldots, \eta_K\right)\mathbf{W}\mathbf{W}^H\right\} \le P_B, \tag{20e}$$

$$\eta_i \ge 0,\ p_i \ge 0,\ \Omega_i \ge 0,\ \forall i \in \mathcal{K}_{\text{R}}. \tag{20f}$$

Problem (20) is hard to solve due to the non-convexity of the objective function (20a) and constraints (20b) and (20c). Let us define $\boldsymbol{\eta}^{(r)}$ and $\boldsymbol{p}^{(r)}$ as the given power coefficients from the $(r-1)$th iteration where $\boldsymbol{\eta}^{(r)} = \left[\eta_1^{(r)}, \ldots, \eta_N^{(r)}\right]^T$, $\boldsymbol{\Omega}^{(r)} = \left[\Omega_1^{(r)}, \ldots, \Omega_N^{(r)}\right]$, and $\boldsymbol{p}^{(r)} = \left[p_1^{(r)}, \ldots, p_N^{(r)}\right]^T$. For the objective function (20a), we can derive an upper bound for the concave function $\mathcal{R}_{j,2}(\boldsymbol{p},\boldsymbol{\Omega})$ at a given point $(\boldsymbol{p}^{(r)}, \boldsymbol{\Omega}^{(r)})$, which is given by

$$\mathcal{R}_{j,2}(\boldsymbol{p},\boldsymbol{\Omega}) \le \sum_{i \in \mathcal{K}_{\text{R}} \setminus \{j\}} E^{(r)}_{j,i}(p_i - p_i^{(r)}) + \sum_{i \in \mathcal{K}_{\text{R}}} E^{(r)}_{j,i}(\Omega_i - \Omega_i^{(r)}) + F_j^{(r)} \triangleq \mathcal{R}^{\text{ub}}_{k,2}(\boldsymbol{p},\boldsymbol{\Omega}),\ \forall k \in \mathcal{K}_{\text{U}}, \tag{21}$$

where $E^{(r)}_{j,i} = \frac{|h_{ij}|^2 \log_2 e}{\sum_{k \in \mathcal{K}_{\text{R}} \setminus \{j\}} p_k^{(r)} |h_{kj}|^2 + \sum_{k \in \mathcal{K}_{\text{R}}} \Omega_k^{(r)} |h_{kj}|^2 + \sigma_U^2}$ and $F_j^{(r)} = \log_2\left(\sum_{k \in \mathcal{K}_{\text{R}} \setminus \{j\}} p_k^{(r)} |h_{kj}|^2 + \sum_{k \in \mathcal{K}_{\text{R}}} \Omega_k^{(r)} |h_{kj}|^2 + \sigma_U^2\right)$ are constants. Similarly, the right-hand-side of constraint (20c) has the following upper bound at the point $(\boldsymbol{p}^{(r)}, \boldsymbol{\Omega}^{(r)})$

$$f_{\text{compress},i}(p_i, \Omega_i) \le \frac{\log_2 e}{p_i^{(r)} + \Omega_i^{(r)}}(p_i + \Omega_i) + \log_2\left(p_i^{(r)} + \Omega_i^{(r)}\right) - \log_2 e - \log_2(\Omega_i) \triangleq f^{\text{ub}}_{\text{compress},i}(p_i). \tag{22}$$

For constraint (20b), the lower bound for $f_{\text{front},i}(\boldsymbol{\eta})$ with respect to $\boldsymbol{\eta}$ using the first-order Taylor expansion at $\boldsymbol{\eta}^{(r)}$ is

$$f_{\text{front},i}(\boldsymbol{\eta}) \ge \log_2\Big(\sum_{k \in \mathcal{K}_{\text{R}}} \left|\boldsymbol{g}_i^T \mathbf{w}_k\right|^2 \eta_k + \sigma_R^2\Big) - \sum_{k \in \mathcal{K}_{\text{R}} \setminus \{i\}} U^{(r)}_{i,k}(\eta_k - \eta_k^{(r)}) - V_i^{(r)} \triangleq f^{\text{lb},2}_{\text{front},i}(\boldsymbol{\eta}), \tag{23}$$

where $U^{(r)}_{i,k} = \frac{\left|\boldsymbol{g}_i^T \mathbf{w}_k\right|^2 \log_2 e}{\sum_{j \in \mathcal{K}_{\text{R}} \setminus \{i\}} \left|\boldsymbol{g}_i^T \mathbf{w}_j\right|^2 \eta_j^{(r)} + \sigma_R^2}$, and $V_i^{(r)} = \log_2\left(\sum_{k \in \mathcal{K}_{\text{R}} \setminus \{i\}} \left|\boldsymbol{g}_i^T \mathbf{w}_k\right|^2 \eta_k^{(r)} + \sigma_R^2\right)$.

Therefore, using (21)-(23), problem (20) can be recast as

$$\max_{\boldsymbol{\eta},\boldsymbol{p},\boldsymbol{\Omega},\boldsymbol{C}} \quad \min_{j} \ \mathcal{R}_{j,1}(\boldsymbol{p},\boldsymbol{\Omega}) - \mathcal{R}^{\text{ub}}_{j,2}(\boldsymbol{p},\boldsymbol{\Omega}) \tag{24a}$$

$$\text{s.t.} \quad C_i \le f^{\text{lb},2}_{\text{front},i}(\boldsymbol{\eta}),\ \forall i \in \mathcal{K}_{\text{R}}, \tag{24b}$$

$$C_i \ge f^{\text{ub}}_{\text{compress},i}(p_i, \Omega_i),\ \forall i \in \mathcal{K}_{\text{R}}, \tag{24c}$$

(20d), (20e), (20f),

which is a convex problem and hence can be solved iteratively using a standard convex optimization toolbox such as CVX.

C. Iterative Algorithm

Similar to [11], we adopt the block coordinate descent algorithm and the overall solution for problem (10) is given in Algorithm 1. It should be noted that the convergence of Algorithm 1 is guaranteed [11]. Note that in sub-problem 1, we approximate (4) by (15) to simplify constraint (10b), and as a result, the obtained optimal solution for sub-problem 1 may not meet all the conditions in the original problem (10). However, a tighter function (23) for the same constraint is used in sub-problem 2 and thus making sure any ultimate solutions are all feasible for problem (10).

Algorithm 1 Proposed Algorithm for Solving (10)

1: Set $r = 0$ and $\epsilon = 10^{-4}$. Initialize $\mathbf{Q}^{(0)}, \boldsymbol{\eta}^{(0)}, \boldsymbol{p}^{(0)}, \text{and } \boldsymbol{\Omega}^{(0)}$
2: **repeat**
3: Solve problem (19) for given $\left\{\mathbf{Q}^{(r)}, \boldsymbol{\eta}^{(r)}, \boldsymbol{p}^{(r)}, \boldsymbol{\Omega}^{(r)}\right\}$, and denote the optimal solution as $\left\{\mathbf{Q}^{(r+1)}\right\}$.
4: Solve problem (24) for given $\left\{\mathbf{Q}^{(r+1)}, \boldsymbol{\eta}^{(r)}, \boldsymbol{p}^{(r)}, \boldsymbol{\Omega}^{(r)}\right\}$, and denote the optimal solution as $\left\{\boldsymbol{\eta}^{(r+1)}, \boldsymbol{p}^{(r+1)}, \boldsymbol{\Omega}^{(r+1)}\right\}$.
5: Update $r = r + 1$.
6: **until** the change in minimum rate between two consecutive iterations is smaller than ϵ.

IV. Numerical Results

In this section, we assess the performance of the proposed algorithm. We assume that the UAVs are deployed in a rural environment and the UEs are randomly and uniformly distributed within a square area of 1 km^2 where the distance between its center and the BBU is denoted by D. Unless otherwise specified, we consider the following simulation parameters: $M = M_x M_y = 20 \times 20 = 400$, $H_B = 30$m, $H_R = 100$m, $\phi = 30°$, $\lambda = 0.15$m, $\sigma_1 = \sigma_2 = -100$ dBm, $P_B = 1$ W, $P_{R,i} = 0.1$ W $\forall i \in \mathcal{K}_{\text{R}}$, $\xi = -40$ dB, and

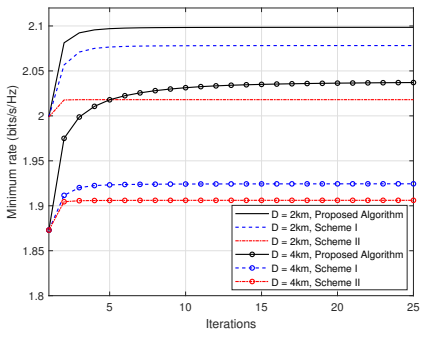

Fig. 2. Convergence speed of the proposed algorithm for $N = 5$ UAV-UE pairs.

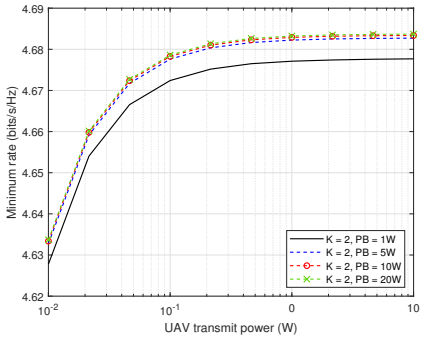

Fig. 3. Minimum rate versus UAVs transmit power for different values of P_B.

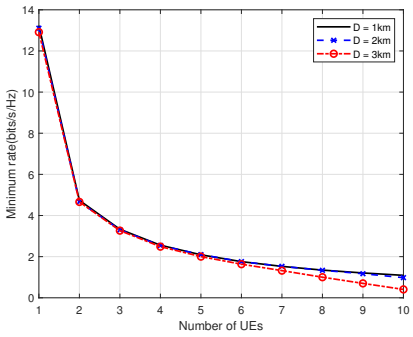

Fig. 4. Minimum rate versus the number of UEs for different values of D.

$d_{\min} = 50$m. The UAVs' locations are initialized above the UEs in Algorithm 1.

Fig. 2 investigates the of the proposed algorithm convergence and illustrates the minimum rate against the iteration number for difference values of D. We consider the scenario of $N = 5$ UAV-UE pairs. For comparison purposes, we consider two benchmark schemes. In the first scheme, referred to as Scheme I, only the placement of UAVs is optimized; and in the second scheme, referred to as Scheme II, only the power control at the BBU and RRH is optimized. We can clearly see that the proposed algorithm significantly outperforms the two benchmark schemes. Also, we notice that as the distance between the BBU and the served area, D, increases from 2 km to 4 km the convergence speeds and achieved minimum rates of the algorithms decrease. We observe that the proposed algorithm and Scheme I have approximately the same convergence speed, which is slower than that of Scheme II.

Fig. 3 demonstrates the impact of the transmit power of UAVs on the minimum rate achieved by each UE for different values of BBU tranmit power. We consider $K = 2$. We can clearly see that as the UAV transmit power increases the minimum rate increases. Also, increasing the BBU transmit power results in improved minimum rate. It is important to notice that as the BBU transmit power increases the rate of improvement of the minimum rate decreases and this can be explained by the fact that beyond a certain value of the BBU tranmit power the access link becomes the bottleneck link.

Fig. 4 shows the performance of the proposed system in terms of average minimum rate versus the number of UEs, N, for different values of D. We can see that the minimum rate drops rapidly with the increased number of UEs. This is because the rate is limited by the interference among UEs in the access link. One solution to improve the performance is to combine the use of multiple antennas and precoding in the access link, which is beyond the scope of the current work and is left as a future work.

V. Conclusion

In this paper, we have proposed a new architecture of multi-UAV-enabled CRAN with a massive MIMO fronthaul link. In particular, we jointly optimized the UAVs placement, power control, and quantization noise variance to maximize the minimum rate of UEs. An iterative algorithm based on the block coordinate descent and successive convex optimization methods was proposed to solve the formulated nonconvex optimization problem. Numerical results showed that our proposed system can significantly increase the minimum rate compared to two benchmark schemes. As a future work, we will use multiple antennas with precoding in the access link to reduce the interference.

References

[1] R. I. Bor-Yaliniz, A. El-Keyi, and H. Yanikomeroglu, "Efficient 3-D placement of an aerial base station in next generation cellular networks," in *2016 IEEE International Conference on Communications (ICC)*, May 2016, pp. 1–5.

[2] M. Mozaffari, W. Saad, M. Bennis, and M. Debbah, "Efficient deployment of multiple unmanned aerial vehicles for optimal wireless coverage," *IEEE Commun. Lett.*, vol. 20, no. 8, pp. 1647–1650, Aug. 2016.

[3] E. Yanmaz, "Connectivity versus area coverage in unmanned aerial vehicle networks," in *2012 IEEE International Conference on Communications (ICC)*, Jun. 2012, pp. 719–723.

[4] S. Hayat, E. Yanmaz, and R. Muzaffar, "Survey on unmanned aerial vehicle networks for civil applications: a communications viewpoint," *IEEE Commun. Surveys Tuts.*, vol. 18, no. 4, pp. 2624–2661, Fourthquarter 2016.

[5] Y. Zeng, Q. Wu, and R. Zhang, "Accessing from the sky: A tutorial on UAV communications for 5G and beyond," *Proceedings of the IEEE*, vol. 107, no. 12, pp. 2327–2375, 2019.

[6] C. Mobile, "C-RAN: the road towards green RAN," *White paper*, vol. 2, pp. 1–10, 2011.

[7] L. Liu, S. Zhang, and R. Zhang, "CoMP in the sky: UAV placement and movement optimization for multi-user communications," *IEEE Trans. Commun.*, vol. 67, no. 8, pp. 5645–5658, Aug. 2019.

[8] S. Roth, A. Kariminezhad, and A. Sezgin, "Base-stations up in the air: Multi-UAV trajectory control for min-rate maximization in uplink C-RAN," in *ICC 2019 - 2019 IEEE International Conference on Communications (ICC)*, 2019, pp. 1–6.

[9] X. Li, C. Pan, C. Zhang, C. He, and K. Wang, "Data rate maximization in UAV-assisted C-RAN," *IEEE Wireless Commun. Lett.*, vol. 9, no. 12, pp. 2163–2167, Dec. 2020.

[10] L. Li, T. Chang, and S. Cai, "UAV positioning and power control for two-way wireless relaying," *IEEE Trans. Wireless Commun.*, vol. 19, no. 2, pp. 1008–1024, 2020.

[11] Q. Wu, Y. Zeng, and R. Zhang, "Joint trajectory and communication design for multi-UAV enabled wireless networks," *IEEE Trans. Wireless Commun.*, vol. 17, no. 3, pp. 2109–2121, Mar. 2018.

[12] S. Park, O. Simeone, O. Sahin, and S. Shamai, "Joint Precoding and Multivariate Backhaul Compression for the Downlink of Cloud Radio Access Networks," *IEEE Trans. Signal Process.*, vol. 61, no. 22, pp. 5646–5658, Nov. 2013.

[13] S. Park, K. Lee, C. Song, and I. Lee, "Joint design of fronthaul and access links for C-RAN with wireless fronthauling," *IEEE Signal Process. Lett.*, vol. 23, no. 11, pp. 1657–1661, Nov. 2016.

[14] M. Grant and S. Boyd, "CVX: Matlab software for disciplined convex programming, version 2.1," http://cvxr.com/cvx, Mar. 2014.